Carbohydrate Polymers 79 (2010) 1028–1033

Contents lists available at ScienceDirect

Carbohydrate Polymers

journal homepage: www.elsevier.com/locate/carbpol

Critical water activity of disaccharide/maltodextrin blends

M. Sillick, C.M. Gregson *

Firmenich Inc., PO Box 5880, Princeton, NJ 08543, USA

ARTICLE INFO

Article history:
Received 2 June 2009
Received in revised form 7 October 2009
Accepted 14 October 2009
Available online 21 October 2009

Keywords:
State diagram
GAB model
Gordon–Taylor model

ABSTRACT

Critical water activity (a_w^*) is employed in this study as a practical metric of the hygroscopic stability of multi-component carbohydrate glasses. Glass transition temperature (T_g) and water activity (a_w) data are modeled to determine the a_w at which sufficient moisture is present to yield a T_g value of 25 °C (i.e., the a_w^*). The results confirm the well-known effect of decreasing sensitivity to moisture with increasing molecular weight. The results also demonstrate the additional influence of molecular type. The hygroscopic stability of binary maltodextrin/disaccharide systems increased in the same order as the glass transition temperature of the disaccharide: sucrose < maltose < trehalose. General equations are proposed for predicting the a_w^* of mixtures, which could be used towards the formulation of stable glassy products.

1. Introduction

Carbohydrate glasses find widespread use in food and pharmaceutical applications. Many food products are stored in the glassy state, e.g., RTE breakfast cereals, milk powder and dehydrated fruit and vegetables. Glasses are frequently used to limit molecular mobility and thereby preserve labile biochemicals (Gouin, 2004). For example, omega-3 fatty acids can be physically encapsulated in glassy carbohydrate matrices by spray drying or melt extrusion (Valentinotti, Armanet, & Porret, 2006). Maintaining appropriate storage conditions at temperatures below the glass transition temperature (T_g) is critical to the success of such products (Franks, 1997; Karel, del Pilar Buera, & Roos, 1993).

Glassy carbohydrate products can fail when exposed to a humid environment due to the plasticising influence of moisture. If sufficient moisture is incorporated, the glass transition can be depressed to below ambient temperature. Depending on the product, this can result in a variety of undesirable consequences, such as caking of particles, collapse of dehydrated structures, loss of crisp textures, crystallization, etc. (Bell & Labuza, 2000). Alternatively, failure or depreciation of quality may occur as a result of increased molecular mobility leading to undesirable chemical reactions or structural rearrangement, such as protein denaturation, at temperatures above T_g (Shamblin, Tang, Chang, Hancock, & Pikal, 1999).

There are a number of ways to assess hygroscopicity. Moisture sorption (i.e., measuring the net weight change of a sample on exposure to humidity) is perhaps the most common approach. However, often it is not necessarily the amount of water absorbed that leads to product failure, but rather the effect of the absorbed water on the mobility and mechanical properties of the glass. The glass transition temperature provides a very useful assessment of the mechanical properties because flow and caking require cooperative rearrangements of the molecular structure and these are limited over relevant time scales at temperatures below T_g. Additionally, molecular mobility can increase by several orders of magnitude as a material is heated through the glass transition (Le Meste, Champion, Roudaut, Blond, & Simatos, 2002). A highly relevant metric of a product's *hygroscopic stability* can therefore be gained by plotting the decrease in T_g with increasing a_w to find the critical water activity (a_w^*) at which T_g approaches 25 °C (Roos, 1993; Zhang, Fan, & Xiao, 2005).

Glass transition temperature and water activity data have been widely reported elsewhere. This work reviews some of the available data to demonstrate the calculation of a_w^*. While the data for pure compounds is plentiful, studies on mixtures or molecular blends of carbohydrates are less common. The goal of the current work is to systematically study the effect of carbohydrate composition on a_w^* for systems in which several materials are blended together. Three disaccharides, sucrose, maltose and trehalose, which have comparatively low molecular weight and therefore low a_w^* values, are blended with maltodextrin polymers (either 18DE or 5DE) and the net a_w^* value is determined based on T_g *vs.* a_w trends. Sucrose and maltose are commonly used in the food industry for making glasses and are often blended with higher molecular weight maltopolymers (e.g., maltodextrin or starch) for such applications (Slade & Levine, 1993). Trehalose is a disaccharide that is receiving increased attention for use in food and pharmaceutical glasses. One advantage of trehalose is that it has the highest T_g of any disaccharide (Imamura, Suzuki, Tatsumichi, Kirii, & Okazaki, 2000).

The DE or dextrose equivalence value is a term which describes the degree of starch hydrolysis in products such as maltodextrin

---

* Corresponding author. Tel.: +1 609 580 6802; fax: +1 609 452 2997.
E-mail address: christopher.gregson@firmenich.com (C.M. Gregson).

0144-8617/$ - see front matter © 2009 Elsevier Ltd. All rights reserved.
doi:10.1016/j.carbpol.2009.10.035

and corn syrup. The DE value describes the number of reducing end groups per 100 units of glucose and is therefore inversely related to the number average molecular weight (M_n). For example, 5DE has a higher M_n than 18DE.

2. Materials and methods

Mixtures of maltodextrin (Star Dri 18 or Star Dri 5, Tate & Lyle, Decatur, IL, USA) and disaccharide (pure cane extra fine granular sucrose, Domino Foods Inc., Yonkers, NY, USA; maltose monohydrate, Alfa Aesar, Ward Hill, MA, USA; or Ascend® trehalose dihydrate, Cargill Inc., Wayzata, MN, USA) were prepared at various ratios on an anhydrous mass basis. The powder mixtures were rendered into a slurry by adding a small amount (approximately 30 wt%) of deionised water. This, in turn, was heated to yield clear concentrated solutions. Moisture content was then decreased (from 30% to 5%) by boiling the solutions within a microwave oven as described by Seo, Oh, Kim, Kim, and Hwang (2004). Aliquots were collected periodically to provide a series of concentrated samples over a range of moisture contents.

Calorimetric measurements were made using a TA Instruments (New Castle, DE, USA) Q200 DSC calibrated for temperature based on the melting point of indium. Samples from each aliquot were prepared and measured in triplicate. The midpoint glass transition temperature was taken as the heat capacity inflection point after rapid quenching from 100 °C (well above T_g). The heating rate was 10 °C/min from −80 °C to 100 °C. This protocol will produce slightly higher T_g and a_w^* values compared to those based on onset T_g.

Water activity was measured at 25 °C with an Aqualab Series 3 meter (Decagon Devices Inc., Pullman, WA, USA), which uses a dew point sensor. Samples were crushed when glassy or mixed when liquid immediately before analysis to create fresh surface. Standard salt solutions supplied by the manufacturer were used to calibrate and monitor the performance of the meter prior to the measurements. Water activity and glass transition temperature data were modelled using the Solver add-in within Excel (Microsoft Corp., Redmond, WA, USA). The model and model parameters are described later. The a_w^* values of each carbohydrate composition were then calculated as the a_w that yields a T_g value of 25 °C. Confidence in the calculated a_w^* was determined as $\sqrt{SS_{\text{error}}/n}$: the square root of the sum of squares of the residuals (i.e., measured − modelled values of a_w) divided by the number of samples.

The number average molecular weight (M_n) of the maltodextrins was measured by freezing point osmometry using the method described by Rong, Sillick, and Gregson (2009). This was done using a μ-Osmette 5400 freezing point osmometer (Precision Systems Inc., Natick, MA, USA) at concentrations of approximately 20 wt% solute. The mole fraction of the chosen disaccharide within the blends was then calculated based on the osmometry result and by assuming a value of 342 g/mol for the disaccharides.

3. Results and discussion

3.1. Calculation of a_w^* and the state diagram approach

Moisture sorption will both increase the a_w and decrease the T_g of a glassy material in well studied ways. Fig. 1 illustrates results for a 15DE maltodextrin sample, which have been fit by the Gordon–Taylor (Eq. (1)) and GAB (Eq. (2)) expressions. These are widely employed equations which describe the T_g and a_w, respectively, of carbohydrate/water systems as well as many other mixtures. Eq. (1) models the T_g of a mixture of two components with weight fractions w_1 and w_2 and glass transition temperatures T_{g1} and T_{g2} using the model constant k. Although this model constant can be calculated theoretically, it is usually treated as an empirical fitting parameter (Palzer, in press; Shamblin, 1997). Eq. (2) relates moisture content (m) to water activity through the model parameters m_m, K, and C, each of which can take physical significance (Normand & Bouquerand, 2007). For example, m_m is often referred to as the monolayer moisture content.

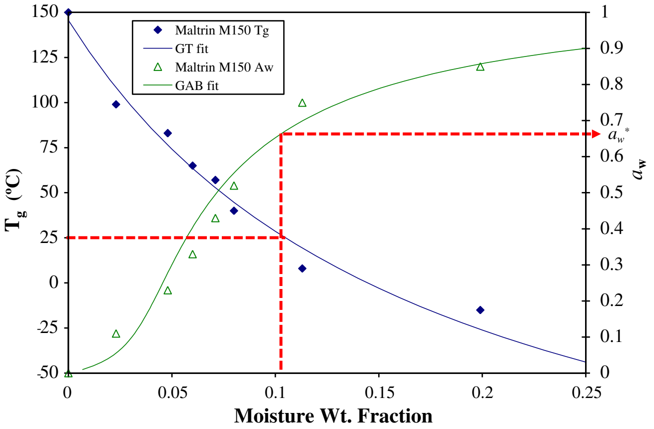

Fig. 1. Trends of T_g and a_w *vs.* moisture content for Maltrin M150 maltodextrin (Roos & Karel, 1991). a_w^* can be derived from the water activity for a composition with a T_g of 25 °C, as illustrated by the dashed lines.

$$T_g = \frac{w_1 T_{g1} + k w_2 T_{g2}}{w_1 + k w_2} \qquad (1)$$

$$\frac{m}{m_m} = \frac{K C a_w}{(1 - K a_w)(1 - K a_w + C K a_w)} \qquad (2)$$

This state diagram approach defines the glass transition and moisture sorption trends as the boundaries between stable and unstable storage conditions (Levine & Slade, 1992). Materials are described as stable (i.e., remain in the glassy state) when stored at temperatures below their T_g and at a relative humidity of less than the $a_w \times 100$. The dashed lines in Fig. 1 illustrate the process of finding the composition that has a T_g of 25 °C based on the Gordon–Taylor trend and subsequently determining a_w^* based on the GAB trend.

Given the well-known relationships illustrated in Fig. 1, it is not surprising that plots of T_g *vs.* a_w (Fig. 2) also progress with smooth and similarly shaped trends. All compositions have their highest T_g at an a_w of 0 (i.e., when anhydrous). The subsequent decrease in T_g at higher a_w values is then typically sigmoidal, though it can show linear dependence through a large range of a_w relevant to the storage of food and pharmaceutical products (Roos & Karel, 1991). These similarities are appealing because they allow one to get some sense of relative hygroscopic stability from a single point on the T_g *vs.* a_w plot.

3.2. Reported a_w^* values for pure carbohydrates and blends

While both glass transition temperatures and water activities of carbohydrate glasses are widely reported in the literature, reducing such data to a critical water activity value is a less common practice. The a_w^* values cited in Table 1 were taken directly from the published source whenever possible. For other cases, the published T_g and a_w data have been replotted and fit using GAB and Gordon–Taylor models to calculate the a_w^* value. Here, GAB expressions for $(1 - m)$ and m were substituted for w_1 and w_2, respectively, in the Gordon–Taylor equation to create a one-step model.

Among those that have promoted the concept of critical water activity are Roos and Karel (1991), who described the glass

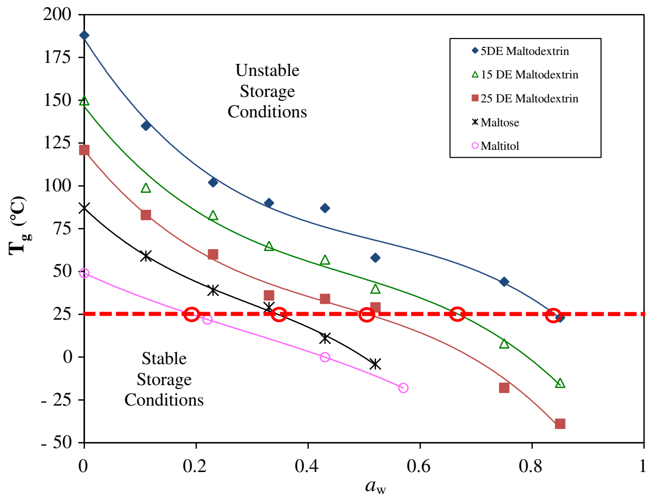

Fig. 2. Plot of T_g *vs.* a_w for several maltodextrin polymers and maltose (Roos & Karel, 1991) and maltitol (Celeghin & Rubiolo, 2006). Trends lines are from a combined Gordon–Taylor and GAB model. a_w^* can be derived as the water activity for a composition with a T_g of 25 °C, which is illustrated by the dashed line. Glasses must be stored at $T < T_g$ and RH < $a_w \times 100$ to maintain stability.

transition trends of a series of maltodextrin polymers conditioned to a range of water activities over saturated salt solutions. Some data from their work is displayed in Figs. 1 and 2. These data clearly show the steady increase in a_w^* with increasing molecular weight.

Other results in Table 1 show that while a_w^* increases with molecular weight for homologous maltopolymers, large differences also exist for different types of carbohydrate. For example, sucrose and trehalose, which share the same chemical formula and molecular weight, have very different a_w^* values (~0.25 and 0.37, respectively).

A study of a maltopolymer–maltose blend was made by Ubbink, Giardiello, and Limbach (2007). While Ubbink et al.'s work focused on specific sorption mechanisms in the glassy state compared to the rubbery state, several sets of a_w^* values were also provided. The a_w^* was shown to increase steadily with increasing average molecular weight (i.e., decreasing maltose fraction). When plotted as a function of maltose weight fraction (Fig. 4A), there is an upwardly concave trend with most of the decrease in a_w^* occurring with the inclusion of the first 40% of the maltose. At a composition of 50% maltose/50% maltopolymer, the a_w^* is 0.44, which is much closer to that of maltose (0.31) than that of the maltopolymer (0.91). This data set is referred to hereafter as "*Maltopolymer/Maltose*" and is included in some of the later modelling exercises.

Foster, Bronlund, and Paterson (2006) studied blends of lactose with small amounts (10 or 20 wt%) of monosaccharide (fructose, galactose, and glucose). Despite the moderately low concentrations of monosaccharide, the resulting T_g *vs.* a_w trends are significantly depressed. Unfortunately, interpretation of these results is hindered because small amounts of crystalline materials were observed. Therefore, the precise composition cannot be known. Nonetheless, it appears from this data that the trend lines of a_w^* *vs.* monosaccharide mass fraction will be steep with small additions of the monosaccharide.

Bouquerand, Maio, Meyer, and Normand (2008) applied a variant of the Gordon–Taylor model and the GAB model to data attained through dynamic vapour sorption and calorimetry. The results show a steep decline in a_w^* when maltodextrin is blended with small amounts of propylene glycol and a more modest decline when blended with maltose.

3.3. Mixtures of 5DE maltodextrin, 18DE maltodextrin, and sucrose

The trends of glass transition temperature *vs.* water activity from several carbohydrate blends prepared for the current work are displayed in Fig. 3. Glass transition temperature is a very strong and approximately linear function of water activity in most cases. The experimental range did not cover very high or low a_w regions, where the trends are expected to become sigmoidal. The gradients

Table 1
a_w^* values reported for carbohydrate glasses.

Glass composition	a_w^*	Theoretical molecular weight	Comment/source
Fructose	<0	180	Anhydrous T_g ~10 °C (Roos & Karel, 1993)
Glucose	Low	180	Anhydrous T_g ~30 °C (Roos & Karel, 1993)
Citric acid	<0	192	Anhydrous T_g 6°C (Maltini, Torreggiani, Venir, & Bertolo, 2003)
Malic acid	<0	134	Anhydrous T_g −21 °C (Maltini et al., 2003)
90% Lactose/10% fructose	*0.23*	314	Foster et al. (2006)
80% Lactose/20% galactose	*0.22*	290	Foster et al. (2006)
80% Lactose/20% glucose	*0.22*	290	Foster et al. (2006)
Sucrose	*0.23*	342	Lechuga-Ballesteros and Miller (2006)
Sucrose	*0.23*	342	Roos and Karel (1993)
Sucrose	*0.26*	342	Imamura et al. (2000)
Maltose	*0.345*	342	Roos and Karel (1993)
Maltose	*0.35*	342	Imamura et al. (2000)
Maltose	0.31	342	Ubbink et al. (2007)
Lactose	0.38	342	Omar and Roos (2007)
Lactose	*0.40*	342	Roos and Karel (1993)
Lactose	*0.39*	342	Imamura et al. (2000)
Lactose	*0.395*	342	Thomsen, Jespersen, Sjostrom, Risbo, and Skibsted (2005)
Trehalose	*0.38*	342	Imamura et al. (2000)
Maltrin M040 (DE 4–7)	0.79	3600	Roos (1993)
Maltrin M100 (DE 9–12)	0.66	1800	Roos (1993)
Maltrin M150 (DE ~15)	*0.68*	1200	Roos and Karel (1991)
Maltrin M200 (DE 20–23)	0.53	900	Roos (1993)
Maltrin M250 (DE 23–27)	0.48	720	Roos (1993)
Maltrin M365 (DE 34–38)	0.39	500	Roos (1993)
Maltodextrin 19DE	0.70	1250	Bouquerand et al. (2008)
Maltodextrin 19DE/20% maltose	0.62	816	Bouquerand et al. (2008)
Maltodextrin 19DE/5% prop. glycol	0.50	767	Bouquerand et al. (2008)

a_w^* values in italics were calculated by the current authors from the reported T_g and a_w data.

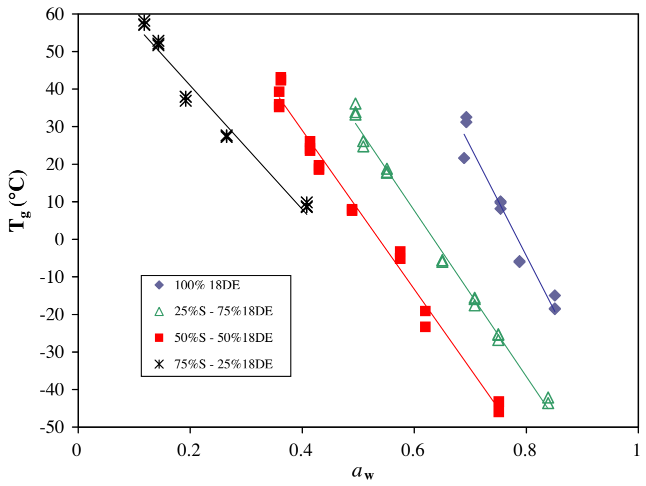

Fig. 3. Trends of T_g *vs.* a_w for selected sucrose/18DE maltodextrin blends.

of different compositions which lie in a similar area of the graph are typically similar, even when comparing compositions made using different DE maltodextrins and/or disaccharide types (data not shown). The negative gradient becomes steeper for compositions that are less sensitive to moisture, i.e., compositions with points lying at higher values of T_g and a_w.

The a_w^* values that correspond to T_g values of 25 °C were extracted from each data set after fitting T_g and a_w data with the model that combined the Gordon–Taylor and GAB equations. Fitting error for the calculation of a_w^* was typically small compared to the differences in a_w^* values between compositions.

The a_w^* of the sample of pure 18DE maltodextrin is 0.70 ± 0.01, which is similar to both Roos and Karel's (1991) value (0.68) for Grain Processing Company Maltrin M150 (15DE) maltodextrin and the results of Bouquerand et al. (2008) for Roquette Glucidex 19DE maltodextrin (0.70). These agreements are reasonable considering the fact that the maltodextrins are from different manufacturers and were analysed by different experimental protocols.

a_w^* values from carbohydrate blends comprised of 18DE maltodextrin and sucrose are shown in Fig. 4A plotted as a function of disaccharide mass fraction. As was the case for Ubbink et al.'s *Maltopolymer/Maltose* data, each trend is upwardly concave. The steepest decline in a_w^* occurs with the addition of small amounts of the lower a_w^* component (i.e., sucrose). At higher concentrations, the a_w^* trend continues to decrease but at a more moderate rate. The trend appears to extrapolate to a value close to that reported for the pure disaccharide.

The a_w^* of 5DE maltodextrin alone is very high (0.83 ± 0.01) and agrees well with Roos and Karel's (1991) data for Grain Processing Company Maltrin M040 (5DE) maltodextrin (0.79). Comparison with the a_w^* of 18DE maltodextrin confirms the expected effect of increasing molecular weight: a_w^* is higher for higher molecular weight maltopolymers (Roos, 1993).

The a_w^* values of the *5DE/Sucrose* blend decrease even more steeply with the addition of sucrose than is the case for the *18DE/Sucrose* blend. This may be expected since the compositions eventually converge at 100% sucrose. However, convergence of the a_w^* trends occurs at a surprisingly low sucrose concentration of approximately 40%. Despite the high molecular weight of 5DE maltodextrin compared to 18DE maltodextrin, the current data set shows no discernable difference in hygroscopic stability when the maltodextrins are blended with sucrose at levels of 40% or more.

3.4. Mixtures of 18DE maltodextrin and other disaccharides

Trends of a_w^* *vs.* disaccharide composition for mixtures of 18DE maltodextrin and sucrose, maltose or trehalose are shown in Fig. 4B. Unlike the maltodextrin:sucrose trends in Fig. 4A, which coincide over much of the range of compositions, the disaccharide blends in Fig. 4B appear well separated and only coincide at a disaccharide fraction near zero. The trend lines lie in the same order as the T_g of the pure disaccharide: sucrose < maltose < trehalose. Additionally, each trend appears to extrapolate to values similar to those reported for the pure disaccharides. Comparison of Fig. 4A and B shows that for mixtures with more than ~25% disaccharide, changing the type of sugar may be a more effective way of increasing a_w^* than using a high molecular weight maltopolymer.

3.5. Modelling of compositional dependence

Fig. 4A and B show the compositional dependence of critical water activity for a number of different blends of disaccharide and

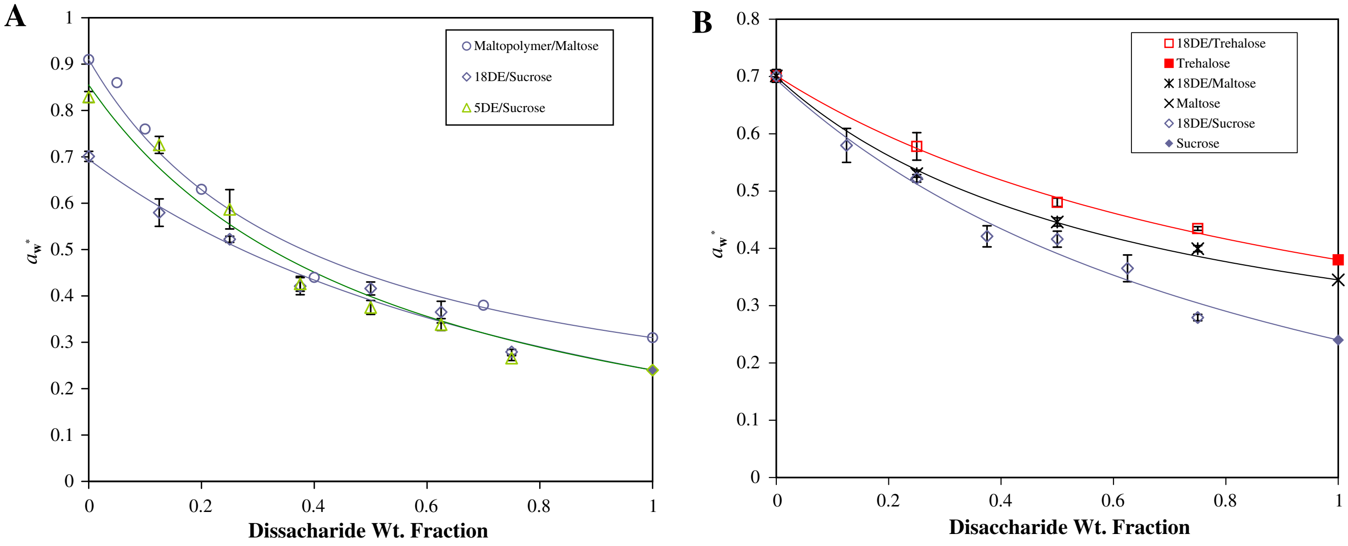

Fig. 4. Trends of a_w^* *vs.* disaccharide weight fraction. (A) Mixtures of sucrose with 5 or 18DE maltodextrin and *Maltopolymer/Maltose*. (B) Mixtures of 18DE maltodextrin and various disaccharides. The a_w^* values of pure disaccharides were taken from the literature: sucrose and maltose (Roos & Karel, 1993), and trehalose (Imamura et al., 2000). The *Maltopolymer/Maltose* trend was also taken from the literature (Ubbink et al., 2007).

maltodextrin. In each case very similar patterns are seen. All of the curves are upwardly concave and appear to connect the a_w^* values of the two constituents of the blend. A simple mixture model with a nonlinearity parameter, such as the modified Gordon–Taylor expression given as Eq. (3) can be successfully applied. Here, a_w^* is the critical water activity of the two component mixture with critical water activities and weight fractions of the pure components a_{w1}^*, w_1 and a_{w2}^*, w_2, respectively.

$$a_w^* = \frac{w_1 a_{w1}^* + \kappa w_2 a_{w2}^*}{w_1 + \kappa w_2} \tag{3}$$

The process of fitting the trends in Fig. 4 by Eq. (3) reveals an interesting relationship between the parameter "κ" and the difference between a_{w1}^* and a_{w2}^*. κ describes the degree of curvature in the trend. Curves with a κ value of unity would appear as a straight line that connects a_{w1}^* and a_{w2}^*. As κ increases above unity, the trend line becomes increasingly nonlinear. For the mixtures considered here, the trends are shown in Fig. 5 to become increasingly curved (i.e., higher κ) with an increase in the difference between a_{w1}^* and a_{w2}^*. The *18DE/Trehalose* mixture has the smallest $a_{w1}^* - a_{w2}^*$ value (0.70–0.38 = 0.32) and also the smallest κ (1.96). The largest difference in a_w^* value within our data is for the *5DE/Sucrose* mixture (0.83–0.23 = 0.60), which also has the largest degree of curvature (κ = 2.87).

Ubbink et al's mixtures of a moderate molecular weight and highly fractionated maltopolymer ($M_w = 1.2 * 10^4$, $M_w/M_n = 2.2$) with maltose represents more purely bidisperse molecular weight distributions than the mixtures used in our work. The fitting result of the *Maltopolymer/Maltose* data shows that while $a_{w1}^* - a_{w2}^*$ is the same as the result from the *5DE/Sucrose* mixture (0.91–0.31 = 0.6), the κ value is considerably larger (3.77 compared to 2.87). This suggests that the molecular weight distribution may have an additional influence on κ.

Alternatively, the molar dependence of a_w^* can be considered, as shown in Fig. 6, by plotting a_w^* as a function of mole fraction. All of the resulting trends are upwardly convex. The degree of curvature can be assessed using an analogous mixing model to that described above by replacing the weight fractions with the mole fractions of the two components, x_1 and x_2, and using κ' to quantify the degree of curvature. Using Eq. (4), κ' takes on values between 0 and 1, with 1 representing a linear trend and degree of curvature increasing with a decrease in value.

$$a_w^* = \frac{x_1 a_{w1}^* + \kappa' x_2 a_{w2}^*}{x_1 + \kappa' x_2} \tag{4}$$

Fig. 7 shows a similar plot to Fig. 5 in which κ' (instead of κ) is represented on the ordinate. Since the *18DE/Maltose* trend is approximately linear on a molar fraction basis (Fig. 6), the resulting κ' value is very close to 1. The relationships in Fig. 7 are similar to those displayed in Fig. 5: mixtures with high curvature again tended to be those which combined materials with very different a_w^* values. Interestingly, the correlation between κ' and $a_{w1}^* - a_{w2}^*$ (mole fraction basis) is significantly better that that with κ (weight fraction basis). This suggests that the mole fraction basis is a more reliable way of estimating curvature, and therefore a_w^*.

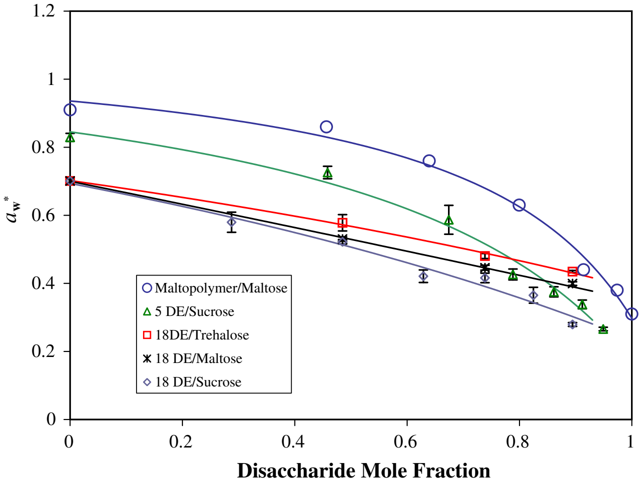

Fig. 6. Trends of a_w^* *vs.* disaccharide mole fraction.

Eqs. (3) and (4) allow the a_w^* of untested carbohydrate mixtures to be predicted based on the a_w^* of their pure components and their weight or mole fractions, respectively. The weight fraction approach has the practical advantage of not requiring molecular weight information, reliable data for which is not always available for carbohydrate polymers. The mole fraction approach has been shown within the current data set to give a better fit of κ' with $a_{w1}^* - a_{w2}^*$. This may allow for a more accurate estimation of a_w^* to be made. Furthermore, in cases where the $a_{w1}^* - a_{w2}^*$ value is less than ~0.35, it appears that very little correction is required for curvature and κ' can be approximated to equal unity.

Taken together, the upwardly concave curvature in Eq. (3) and the upwardly convex curvature for Eq. (4) lay on opposite sides of a linear relationship. That is, the a_w^* value of a mixture lies below that which would be expected based on a straight line connecting the a_w^* values of any two individual components on a weight basis, but above a similarly predicted value on a molar basis. This implies that an alternative average scheme which results in an effective molecular weight between that of M_n and M_w would yield a linear relation with the a_w^* of the mixture.

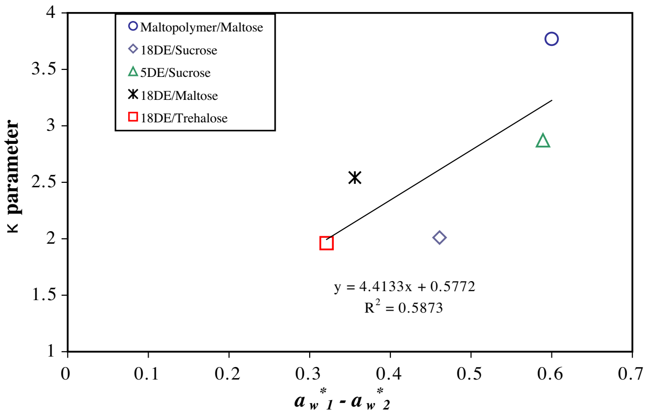

Fig. 5. The curvature parameter "κ" plotted as a function of $a_{w1}^* - a_{w2}^*$ for maltopolymer/disaccharide mixtures.

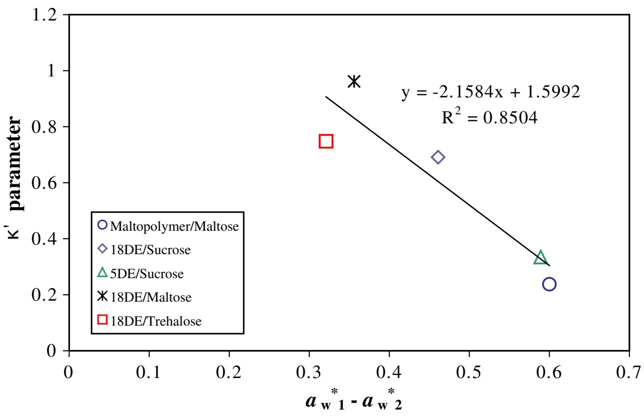

Fig. 7. The mole fraction curvature parameter (κ') plotted as a function of $a_{w1}^* - a_{w2}^*$ for maltopolymer/disaccharide mixtures.

4. Concluding remarks

The results show that the a_w^* of carbohydrates mixtures depends on both molecular weight and the type of molecules that are present. Even among disaccharides, the type of sugar has a significant influence with a_w^* increasing in the order sucrose < maltose < trehalose. a_w^* is controlled in part by glass transition temperatures, which increase significantly in the same order.

While a full understanding of the effect of molecular weight, configuration and molecular weight distribution on κ and κ' has yet to be demonstrated, this work allows for reasonable estimates of the a_w^* of mixtures to be made based on the composition of a mixture and the a_w^* values of pure constituents. This may be useful for controlling the hygroscopic stability of a number of industrially important glassy products.

References

Bell, L. N., & Labuza, T. P. (2000). *Moisture sorption: Practical aspects of isotherm measurement and use*. St. Paul, MN: American Association of Cereal Chemists.

Bouquerand, P.-E., Maio, S., Meyer, F., & Normand, V. (2008). Moisture stability of maltodextrin-based delivery systems. *Food Biophysics, 3*, 182–185.

Celeghin, A. G., & Rubiolo, A. C. (2006). The water content and glass-transition temperature of low calory candy formulations. In M. del Pilar Buera, J. Welti-Chanes, P. J. Lillford, & H. R. Corti (Eds.), *Water properties of food, pharmaceutical, and biological materials* (pp. 703–708). Boca Raton, FL: CRC Press.

Foster, K. D., Bronlund, J. E., & Paterson, A. H. J. (2006). Glass transition related cohesion of amorphous sugar powders. *Journal of Food Engineering, 77*, 997–1006.

Franks, F. (1997). Phase changes and chemical reactions in solid aqueous solutions: Science and technology. *Pure & Applied Chemistry, 69*, 915–920.

Gouin, S. (2004). Microencapsulation: Industrial appraisal of existing technologies and trends. *Trends in Food Science & Technology, 15*, 330–347.

Imamura, K., Suzuki, T., Tatsumichi, S., Kirii, S., & Okazaki, M. (2000). Water sorption and glass transition of amorphous sugars containing BSA. *Journal of Chemical Engineering of Japan, 33*, 657–660.

Karel, M., del Pilar Buera, M., & Roos, Y. (1993). Effects of glass transitions on processing and storage. In J. M. V. Blanshard & P. J. Lillford (Eds.), *The glassy state in foods* (pp. 13–30). Loughborough: Nottingham University Press.

Le Meste, M., Champion, D., Roudaut, G., Blond, G., & Simatos, D. (2002). Glass transition and food technology: A critical appraisal. *Journal of Food Science, 67*, 2444–2458.

Lechuga-Ballesteros, D., & Miller, D. P. (2006). The hydration limit of amorphous solids and long-term stability. In M. del Pilar Buera, J. L. Welti-Chanes, P. J. Lillford, & H. R. Corti (Eds.), *Water properties of food, pharmaceutical, and biological materials* (pp. 303–308). Boca Raton, FL: CRC Press.

Levine, H., & Slade, L. (1992). Glass transition in foods. In H. G. Schwartzburg & R. W. Hartel (Eds.), *Physical chemistry of foods* (pp. 82–222). New York: Marcel Dekker.

Maltini, E., Torreggiani, D., Venir, E., & Bertolo, G. (2003). Water activity and the preservation of plant foods. *Food Chemistry, 82*, 79–86.

Normand, V., & Bouquerand, P.-E. (2007). Dimensionless hygroscopic number of malto-oligomers. *Starch/Starke, 59*, 100–102.

Omar, A. M. E., & Roos, Y. H. (2007). Glass transition and crystallization behaviour of freeze-dried lactose–salt mixtures. *LWT – Food Science and Technology, 40*, 536–543.

Palzer, S. (in press). The relation between material properties and supra-molecular structure of water-soluble food solids. *Trends in Food Science & Technology*. doi:10.1016/j.tifs.2009.08.005. Available from <http://www.sciencedirect.com/science/article/B6VHY-4X7GMDB-1/2/bbe04e999014a3bdcf10de8549ad1a7f>.

Rong, Y., Sillick, M., & Gregson, C. M. (2009). Determination of dextrose equivalent value and number average molecular weight of maltodextrin by osmometry. *Journal of Food Science, 74*, C33–C40.

Roos, Y. (1993). Water activity and physical state effects on amorphous food stability. *Journal of Food Processing and Preservation, 16*, 433–447.

Roos, Y., & Karel, M. (1991). Phase transitions of mixtures of amorphous polysaccharides and sugars. *Biotechnology Progress, 7*, 49–53.

Roos, Y., & Karel, M. (1993). Effects of glass transition on dynamic phenomena in sugar containing food systems. In J. M. V. Blanshard & P. J. Lillford (Eds.), *The glassy state in foods* (pp. 207–222). Loughborough: Nottingham University Press.

Seo, J. A., Oh, J., Kim, D. J., Kim, H. K., & Hwang, Y. H. (2004). Making monosaccharide and disaccharide sugar glasses by using microwave oven. *Journal of Non-Crystalline Solids, 333*, 111–114.

Shamblin, S. L. (1997). *The characteristics of sucrose–polymer mixtures in the amorphous state*. Thesis/Dissertation. University of Wisconsin-Madison.

Shamblin, S. L., Tang, X., Chang, L., Hancock, B. C., & Pikal, M. J. (1999). Characterization of the time scales of molecular motion in pharmaceutically important glasses. *Journal of Physical Chemistry B, 103*, 4113–4121.

Slade, L., & Levine, H. (1993). The glassy state phenomenon in food molecules. In J. M. V. Blanshard & P. J. Lillford (Eds.), *The glassy state in foods* (pp. 35–97). Loughborough: Nottingham University Press.

Thomsen, M. K., Jespersen, L., Sjostrom, K., Risbo, J., & Skibsted, L. H. (2005). Water activity–temperature state diagram of amorphous lactose. *Journal of Agricultural and Food Chemistry, 53*, 9182–9185.

Ubbink, J., Giardiello, M.-I., & Limbach, H.-J. (2007). Sorption of water by bidisperse mixtures of carbohydrates in glassy and rubbery states. *Biomacromolecules, 8*, 2862–2873.

Valentinotti, S., Armanet, L., & Porret, J. (2006). Encapsulated polyunsaturated fatty acids. *US Patent Office*, App. No. 20060134180A1.

Zhang, M., Fan, L., & Xiao, G. (2005). Method for determining storage conditions for glass transition of dried product or deep-fried chip of fruit and vegetable. *State Intellectual Property Office of the P.R.C.*, Patent No. 1676005.